"LONDON"

Radial Profilometry

by

John A. Gilbert
Department of Mechanical Engineering
Center for Applied Optics
University of Alabama in Huntsville
Huntsville, Alabama 35899

Pal Greguss
Applied Biophysics Laboratory
Technical University Budapest
P. O. Box 91
Budapest, Hungary H-1502

David L. Lehner
Department of Mechanical Engineering
University of Alabama in Huntsville
Huntsville, Alabama 35899

Jeffrey L. Lindner
Department of Mechanical Engineering
University of Alabama in Huntsville
Huntsville, Alabama 35899

Abstract

This paper describes a new device, called a radial profilometer, capable of contouring or measuring deflections on the inner surfaces of cavities found for example, inside pipes, tubes, and boreholes. The equations considered in designing and testing a prototype are described along with feasibility tests conducted to illustrate proof of principle. Future research is discussed, including a design for a fiber-based probe from which quantitative measurements are automatically extracted using a computer-based system.

Introduction

Profiling measurements are important in many fields, especially in cases where chemical deposits cause corrosion, or where combinations of thermal and mechanical stresses cause wear or produce cracks. Such conditions are typically encountered in nuclear power plants and in rocket engines where many components, designed to function at high temperatures and pressures, must be periodically inspected to avoid cataclysmic failures. Profiling techniques are also important in industrial manufacturing to identify parts outside of set tolerances, and to pinpoint defective or missing components.

Perhaps the oldest and best known method for profiling is photogrammetry where the basic approach is to photograph an object with one or more precision cameras from different incident angles and then to superimpose these photos to form a three-dimensional image of the object. Deflections experienced by the test object are determined by measuring shifts in the position of its image relative to a known reference point[1]. An alternate approach for profiling is the shadow moire method in which a reference grating is placed in front of the test surface. When illuminated at an oblique angle, the reference grating casts a shadow on the surface, and the shadow deforms as the surface moves relative to the reference grating. The lines of the reference grating superimpose with those in the shadow to form a moire which can be analyzed to determine surface deflection[2].

Improvements have been made in both of these techniques by incorporating optical and image processing equipment for data acquisition and analysis. For

example, Kahn-Jetter and Chu recently introduced a technique based on photogrammetry that combines stereoscopic analysis and digital image correlation techniques[3]. Two sets of stereo images are recorded for an undeformed and deformed test surface painted white and splattered with black paint. Digital image correlation techniques are applied to determine displacement. Sang, Lee, and Chang developed a simple method based on shadow moire for measuring local buckling of thin walled members by projecting a pattern of parallel equispaced lines on a test surface[4]. These lines are tracked by a computer and changes in their locations are related to movements in the out-of-plane direction. Gilbert et al combined the simplicity of shadow moire and the sophistication of photogrammetry in a technique called shadow speckle metrology in which random speckles, projected onto the test surface, are numerically correlated by a computer to profile structural components[5,6]. Optical fibers were later incorporated into shadow speckle metrology to facilitate remote testing[7]. Further improvements were made by Lehner et al for studying dynamic behavior by introducing a technique called line broadening[8]. In that technique, a line is projected at an oblique angle onto a vibrating surface and the resulting image is tracked by a computer. Broadening takes place in areas where motion occurs and quantitative measurements are made to determine displacements.

The profiling techniques described above have been applied mainly to profile the outer surfaces of structural components. In general, these measurement systems rely on a large number of optical and electronic components, many of which are difficult to miniaturize. Although optical fibers offer potential for miniaturization and could be incorporated into such systems to profile remote surfaces, these systems (as well as the more conventional non-fiber-based systems) suffer from a limited field of view. This presents a problem, for example, when profiling the inner wall of a pipe. In this case, the imaging device would have to be translated along, and rotated around, the optical axis of the device to examine all points on the inner surface of the pipe; constraints which severely limit functional and real-time capabilities.

Ideally, a device for profiling the inner surface of a cavity should be rugged, compact, and capable of obtaining an unobstructed, complete, and comprehensive image of the cavity space in every direction. The measurement process should be sophisticated enough to fully characterize the test surface, yet simple enough to allow a technician to make the required measurements easily.

Unfortunately, it is virtually impossible to develop a practical device capable of recording a sphere of vision. However, most cavities can be regarded as cylindrical rather than spherical volumes, and information can be transformed, using stretching methods, onto a flat surface creating a 2-D representation of the 3-D cylindrical surface. This phenomenon called Flat Cylinder Perspective (FCP) forms the basis for a panoramic doughnut lens developed by Greguss at the Applied Biophysics Laboratory in Budapest, Hungary[9]. The lens produces an annular FCP image where the width of annular image corresponds to the vertical viewing angle; each concentric ring in the image plane is the loci of points recorded at a constant horizontal field angle[10]. The lens has been used to make holo-interferometric and speckle photographic recordings[11] and, when combined with the line broadening technique[8], can be used for radial profilometry.

Analysis

Figure 1 shows a cross-sectional view of a device built to demonstrate proof of principle for radial profilometry. An unexpanded beam produced by a laser (1) passes through a 90 degree prism (2) (mounted on a transparent glass plate (4)) and reflects off a rotating front surface mirror (3). The laser beam reflects off the mirror, passes through the glass plate (4), and illuminates the interior wall of a cavity (5). The figure shows a pipe being tested with its longitudinal axis positioned symmetrically with respect to the optical axis of the profilometer. In this case, the laser traces out a circular ring on the inside wall of the pipe. The image of the illuminated surface is captured by the panoramic doughnut lens (6), and is projected by the projection lens (7) onto the image plane of a conventional 35mm camera (8).

Figure 2 defines the cartesian and cylindrical coordinate systems to be used for subsequent analysis. In both systems, the optical axis of the profilometer lies along the z-direction; point S corresponds to the position of the rotating mirror denoted by (3) on Figure 1. Light is projected to point P at an angle α, and the image of the illuminated surface is captured at an angle β, measured with respect to a radial line lying in the r-z plane. When the surface moves relative to the optical axis, the projected image appears to shift along the z-direction through a displacement w. The corresponding radial displacement, r, is given by

$$r = \frac{w}{\tan [90 - \alpha] + \tan \beta} \qquad (1)$$

The relationship between r and w is nonlinear, since β varies from point to point.

The displacement along the z-direction is mapped into the image plane by the panoramic doughnut lens via a mapping function, f, as follows

$$r' = f[w] \qquad (2)$$

This function takes into account the magnification factor, and includes the FCP stretching methods used to create a 2-D representation of the 3-D cylindrical surface. Ideally, one would like to design a radial profilometer so that the nonlinear effects inherent in Equations (1) and (2) compensate one another over as large a range as possible, such that,

$$r' = Cr + b \qquad (3)$$

where C and b are constants.

By measuring r' and knowing C and b, Equation (3) can be solved for r. Once r is established for a known value of θ, the z-coordinate of the illuminated point can be calculated using,

$$z = \frac{r}{\sin \alpha} \qquad (4)$$

Therefore, one procedure for profiling a cavity is to initially establish a fixed global axis system in space with its z-axis aligned with that of the local system shown in Figure 2, and then to move the profilometer along the z-direction. The coordinates for r and θ are the same for the local and global systems; z-coordinates in the global system are calculated by taking into account the relative position of the local system.

Experimental

A radial profilometer was designed and built to satisfy the condition in Equation (3). The device was tested as shown in Figure 1 by inserting it into a circular pipe with an inner radius, R, equal to 2.25" (57.2 mm). The optical axis of the profilometer was positioned parallel to the longitudinal axis of the pipe; the coordinate system shown in Figure 2 was used for analysis.

Figure 3 shows the image photographed when the radial profilometer is positioned at the center of the pipe. The relatively thick circle is the laser trace; thin equispaced lines were drawn on the interior surface of the pipe to visually illustrate the nonlinear mapping inherent in Equation (2).

Figure 4 was recorded after the pipe was translated along the x-direction through a displacement, u, of 0.35" (8.9 mm). Radial lines, drawn every five degrees, were superimposed on the photograph to aid in calibrating the profilometer. With θ measured from x,

$$r = \left[u^2 + R^2 + 2uR \cos (\theta + \gamma) \right]^{1/2} \qquad (5)$$

where R is the inner radius of the pipe, and $\gamma = \sin^{-1} [(u \sin \theta)/R]$.

Equation (5) can be derived using simple geometry, and defines the radial distance between the pipe and the optical axis of the profilometer for any angle θ. More importantly, the equation holds for any z-coordinate, since the optical axis of the device remains parallel to the longitudinal axis of the pipe and the cross section of the pipe is constant. This makes the translated pipe ideal for calibrating the profilometer, since r' can be measured on Figure 4.

Figure 5 shows the calibration curve established by plotting r [calculated on

the basis of Equation (5)] versus r' [measured along the radial lines superimposed on Figure (4)] for points taken at five degrees increments as θ ranged from 0 to 360 degrees. The curve holds over a 0.70" (17.8 mm) range where the value of r lies between 1.9" (48.26 mm) and 2.6" (66.04 mm). In this range, the response is linear and governed by Equation (3) with C equal to 2.06. A value of b = - .71" (-18 mm) is established by interpolating the curve back to r = 0. No physical interpretation can be associated with this value of b (r' at r = 0), since the central portion of the PDL contains no image. It is simply one of the parameters required in Equation (3) to evaluate r within the calibrated range.

Further tests were conducted for several translations along the x-direction, ranging in magnitude from 0 to 0.35" (8.9 mm). Figure 6 shows a plot of displacements observed on the micrometer stage used to translate the pipe relative to the device versus experimental data taken using the profilometer and Equation (3) for θ = 0. The solid line shows the "ideal" response.

Finally, Figure 7 shows the result of placing several inclusions of constant cross section on the inner wall of the pipe. In this case, the laser maps out shapes in the image plane which are "similar" to those of the inclusions. Each shape is reduced (or magnified) in size as defined by the constant, C, in Equation (3).

Discussion

The device shown in Figure 1 has some major drawbacks which limit its potential for practical application. A practical device should be packaged so that it can be easily manipulated throughout a cavity. Analysis should be automated with a minimal amount of response time.

Figure 8 is a schematic of one of many optical configurations currently being evaluated for radial profilometry. The radial profilometer is shown inserted into a cylindrical cavity. A diverging laser beam (shown launched from a fiber optic labeled 1) is directed through a projection lens (2). The beam passes through a panoramic doughnut lens (3) and is collimated and shaped by an appropriately masked collimating lens (4) to produce a thin ring. The ring reflects off a conical mirror (5) and passes through a transparent window (6) onto the test surface (7). The image of the illuminated surface is captured through the transparent window (6) by the panoramic doughnut lens (3) and is projected by the projection lens (2) onto a coherent optical fiber bundle (8). The bundle further transmits the image from the device to a photoelectronic-numerical processing system where changes in the image are recorded and analyzed using standard image acquisition and computer processing techniques.

The advantages of this device are that it is simple and relatively inexpensive, it can be miniaturized, there are no moving parts, the image is continuously displayed in the image plane, and measurements are completely automated. Future publications will discuss the advantages and disadvantages of this and other configurations proposed for radial profilometry. The range and accuracy for each configuration will be presented. Examples of practical applications will be given along with appropriate discussions of the numerical algorithms and computer software used to automatically extract quantitative

measurements from the observed shifts in the position of the image.

Conclusion

This paper has described a new device, called a radial profilometer, capable of contouring or measuring deflections on the inner surfaces of cavities found for example, inside pipes, tubes, and boreholes. An alalysis has been presented which demonstrates that an entire cavity can be profiled simply by moving such a device through the cavity. Feasibility tests have shown that the profilometer can be designed so that information is extracted based on a linear calibration curve. Guidelines have been established for further development including automated analysis, and one of the designs currently under evaluation for practical implementation has been described in detail.

Acknowledgement

The authors wish to acknowledge support provided by the Center for Applied Optics at the University of Alabama in Huntsville and the Applied Biophysics Laboratory at the Technical University Budapest. Mr. Lehner and Mr. Lindner are funded as research assistants by the U.S. Army Research Office in Research Triangle Park, N.C. under contract number DAAL 03-86-K-0014.

References

1. Gates, T.S., Photogrammetry as a means of mapping postbuckled composite surfaces, Experimental Techniques 10(6), (1986), pp. 18-22.

2. Pirodda, L., Shadow and projection moire techniques for absolute or relative mapping of surface shapes, Optical Engineering 21(4), (1982), pp. 640-649.

3. Kahn-Jetter, Z.L., Chu, T.C., The use of digital image correlation techniques and stereoscopic analysis for the measurement of deformations on a warped surface, Proceedings of the SEM Spring Conference on Experimental Mechanics, New Orleans, June 8-13, 1986, pp. 820-826.

4. Sang, Z.T., Lee, G.C., Chang, K.C., A simple method for measuring local buckling of thin-walled steel members, Proceedings of the SEM Spring Conference on Experimental Mechanics, New Orleans, June 8-13, 1986, pp. 464-469.

5. Gilbert, J.A., Matthys, D.R., Taher, M.A., Petersen, M.E., Shadow speckle metrology, Applied Optics 25(2), (1986), pp. 189-203.

6. Gilbert, J.A., Matthys, D.R., Taher, M.A., Petersen, M.E., "Profiling structural members using shadow speckle metrology," accepted for publication in Optics and Lasers in Engineering, 1987.

7. Gilbert, J.A., Matthys, D.R., Taher, M.A., Petersen, M.E., Remote shadow speckle metrology, Proceedings of the SEM Spring Conference on

Experimental Mechanics, New Orleans, June 8-13, 1986, pp. 814-818.

8. Lehner, D.L., Dudderar, T.D., Matthys, D.R., Gilbert, J.A., Vibration analysis using shadow speckle metrology and line broadening techniques, Proceedings of the SEM Spring Conference on Experimental Mechanics, Houston, Texas, June 14-19, 1987.

9. Greguss, P., U.S. Patent No. 4,566,763, 1984.

10. Greguss, P., The tube peeper: a new concept in endoscopy, Optics and Laser Technology 17, (1985), pp. 41-45.

11. Greguss, P., Panoramic holocamera for tube and borehole inspection, International Seminar on Laser and Optoelectronic Technology in Industry - A State of Art Review, June 25-27, 1986, Xiamen, P.R.C.

List of Figures

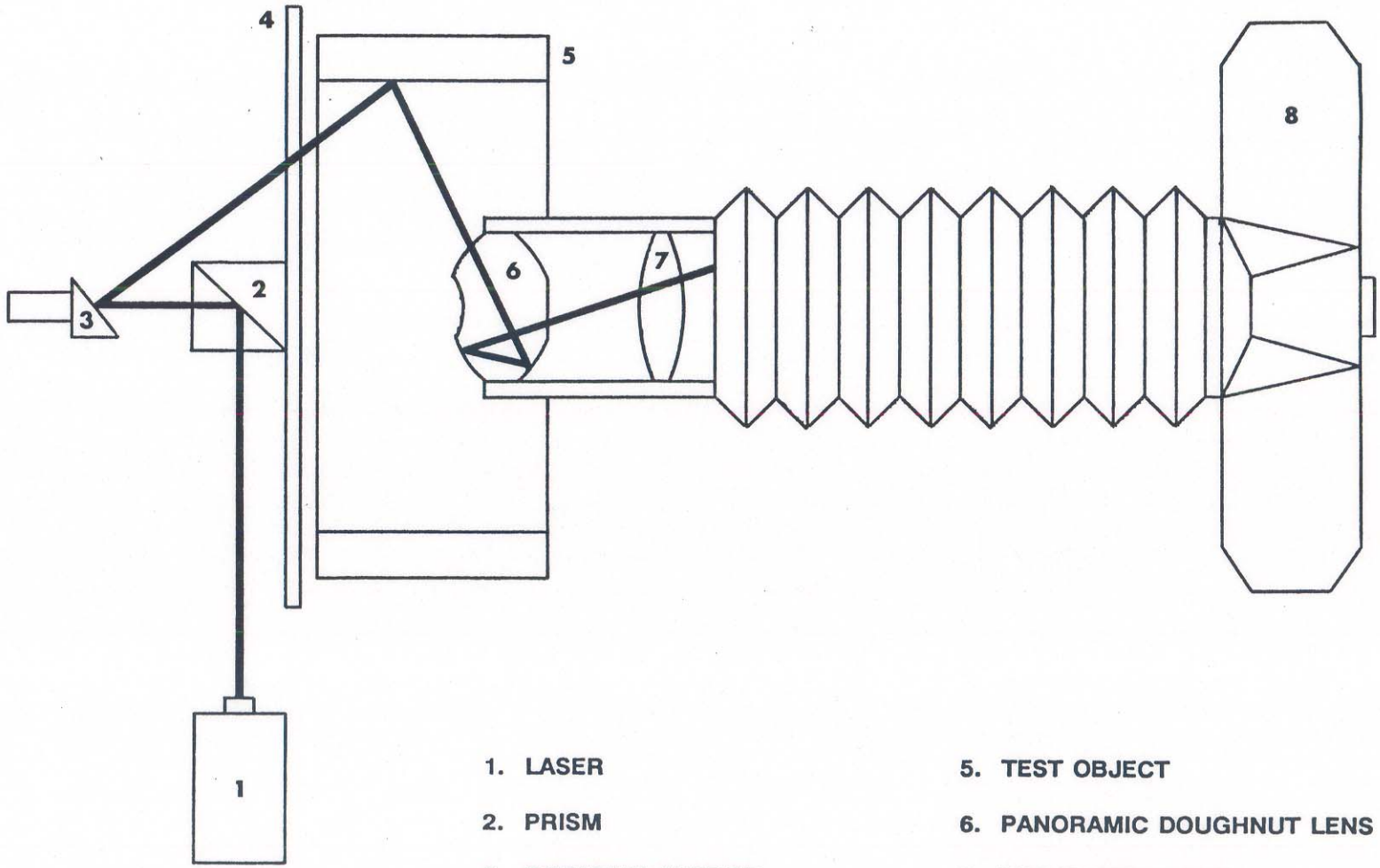

1. LASER
2. PRISM
3. ROTATING MIRROR
4. GLASS MOUNTING PLATE
5. TEST OBJECT
6. PANORAMIC DOUGHNUT LENS
7. PROJECTION LENS
8. 35mm CAMERA BODY

Figure 1

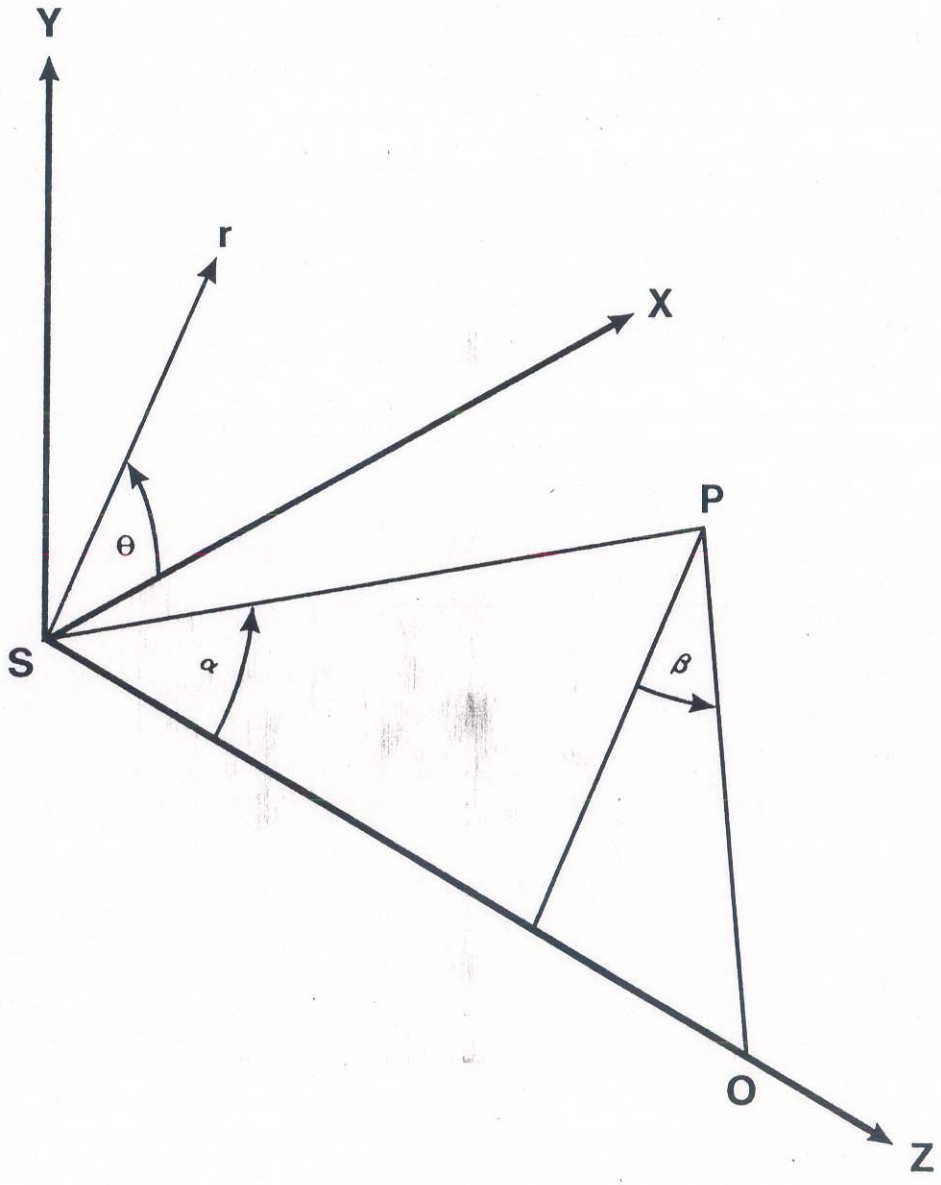

Figure 2

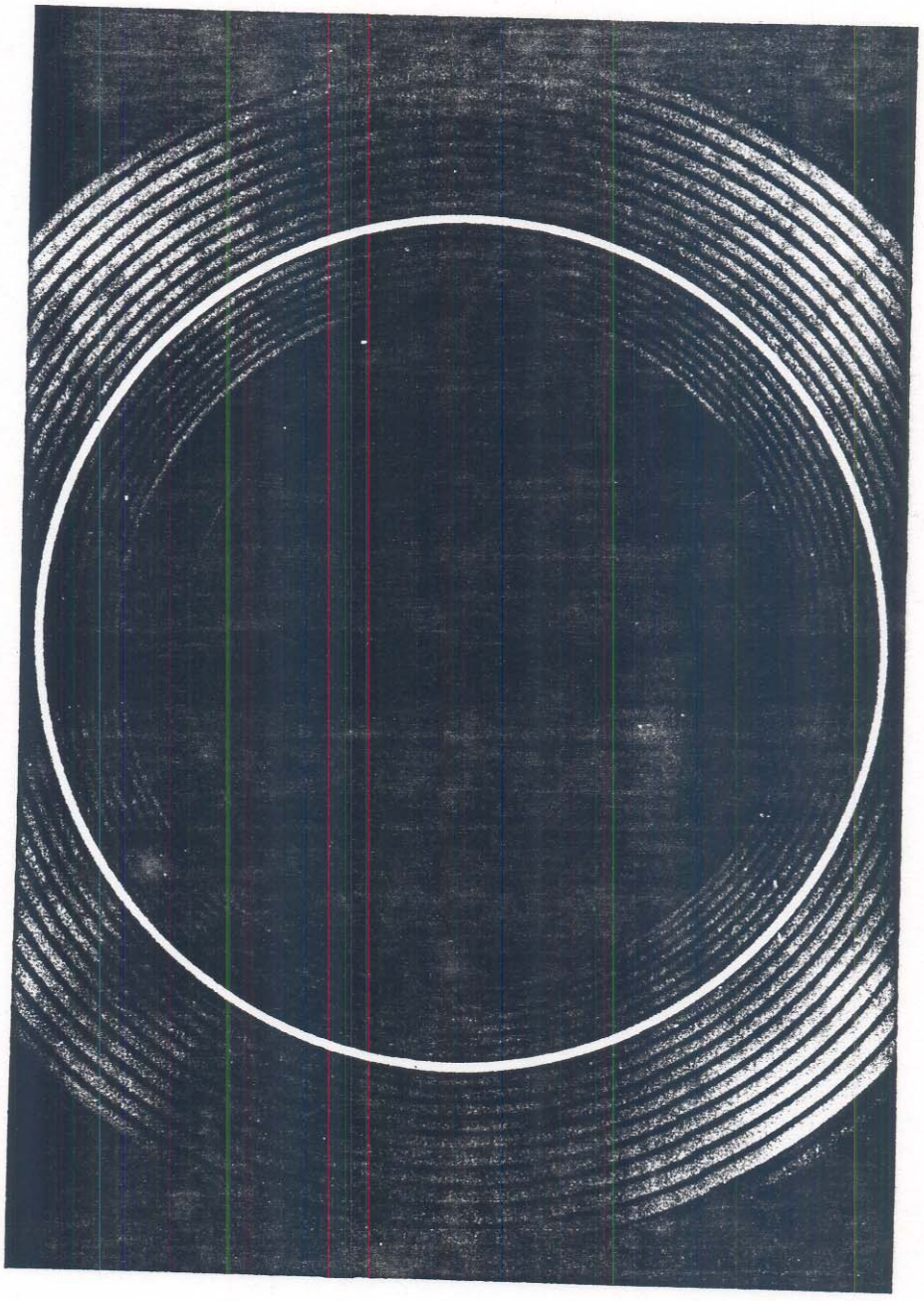

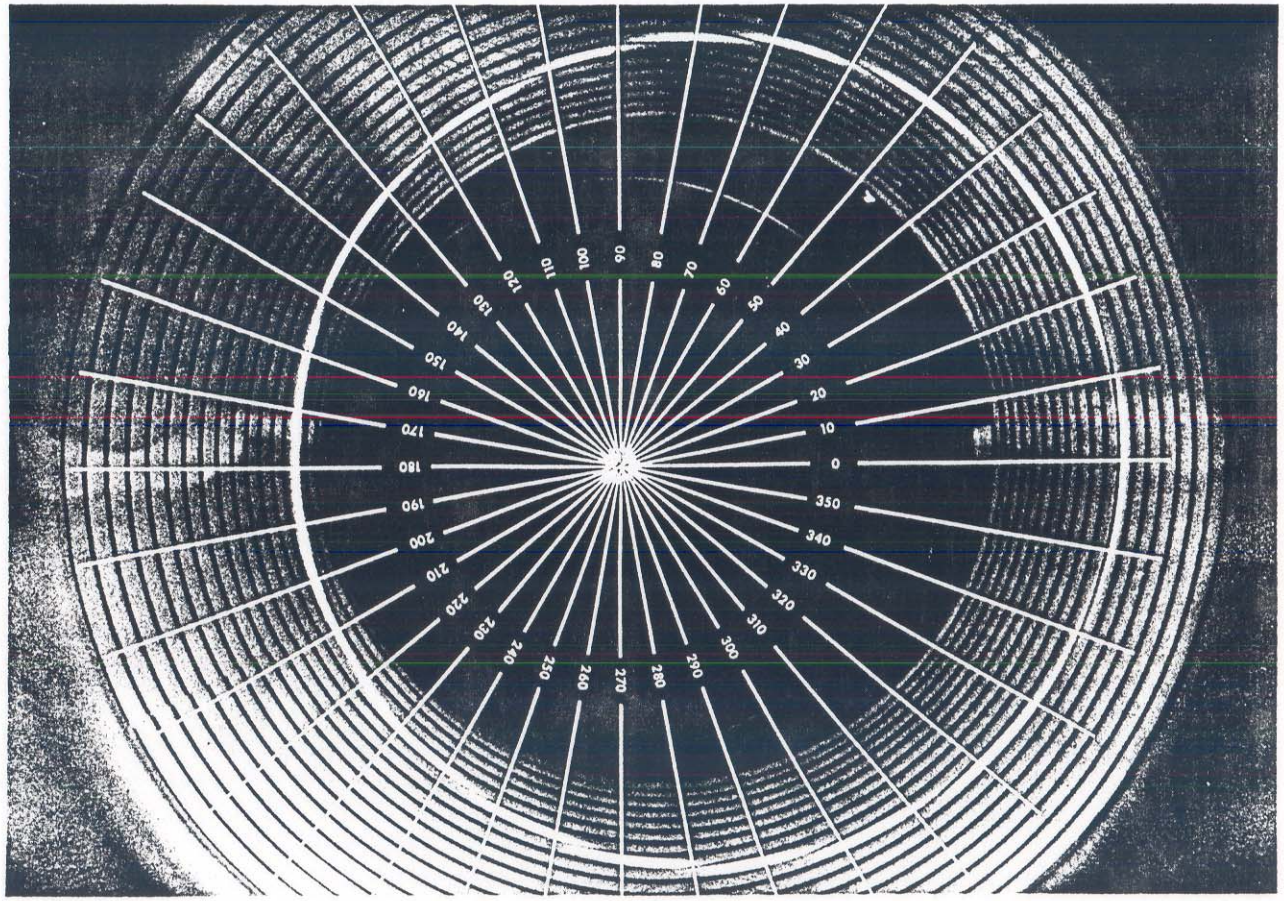
90
80
70
60
50
40
30
20
10
0
350
340
330
320
310
300
290
280
270
260
250
240
230
220
210
200
190
180
170
160
150
140
130
120
110
100

Figure 4.

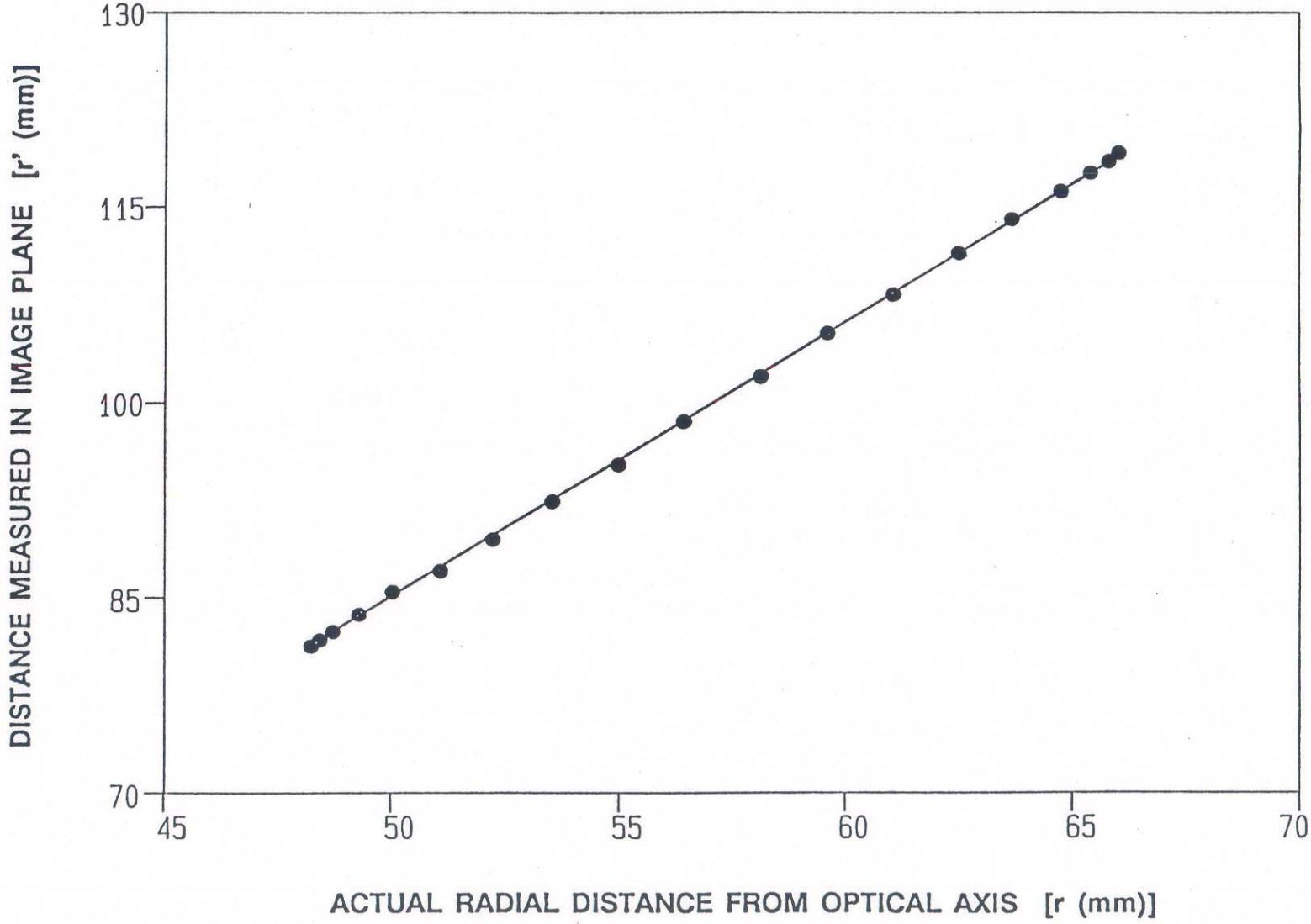
130
115
100
85
70
45
50
55
60
65
70
DISTANCE MEASURED IN IMAGE PLANE [r' (mm)]
ACTUAL RADIAL DISTANCE FROM OPTICAL AXIS [r (mm)]

Figure 5

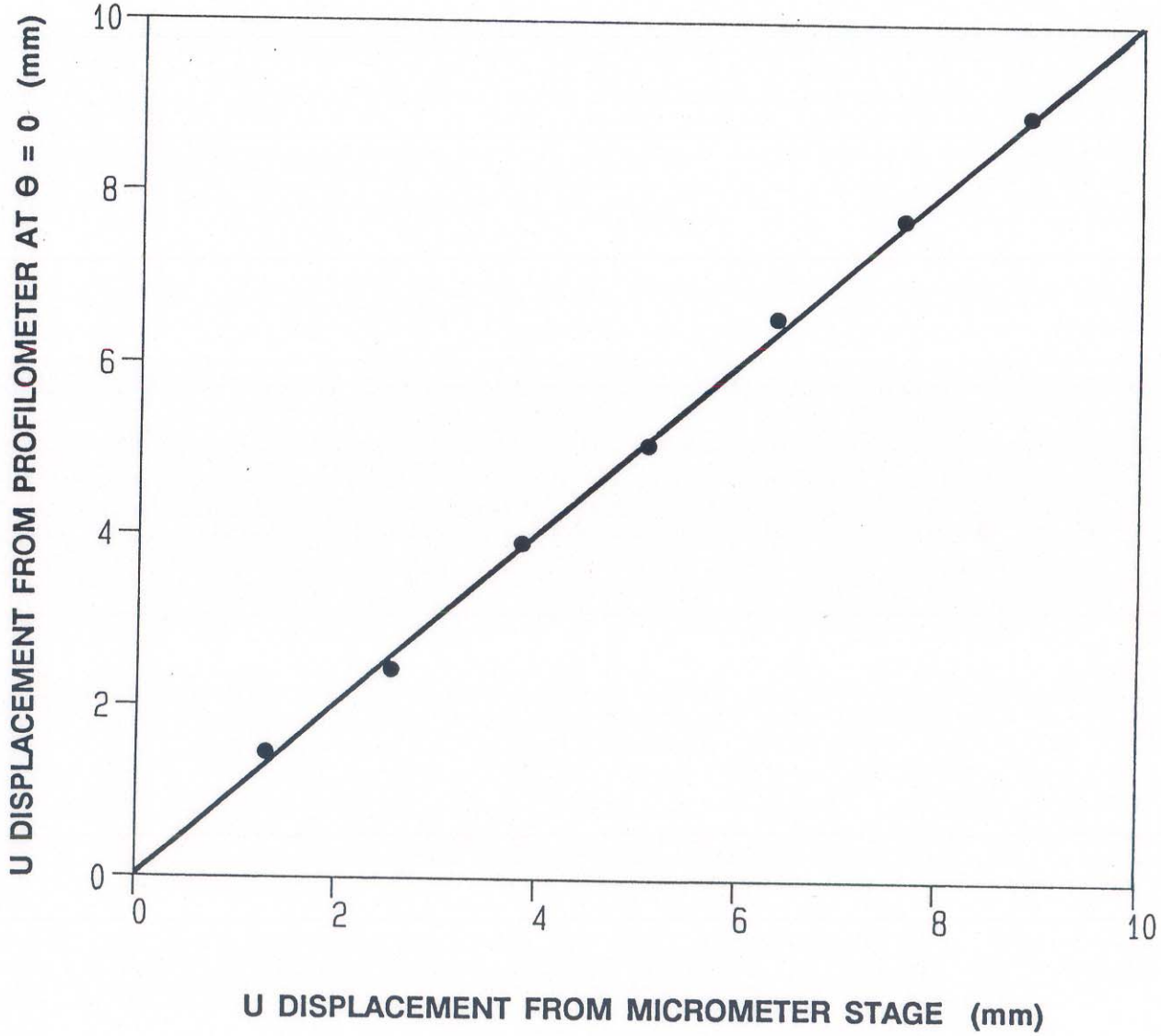
U DISPLACEMENT FROM PROFILOMETER AT Θ = 0 (mm)
10
8
6
4
2
0
0
2
4
6
8
10
U DISPLACEMENT FROM MICROMETER STAGE (mm)

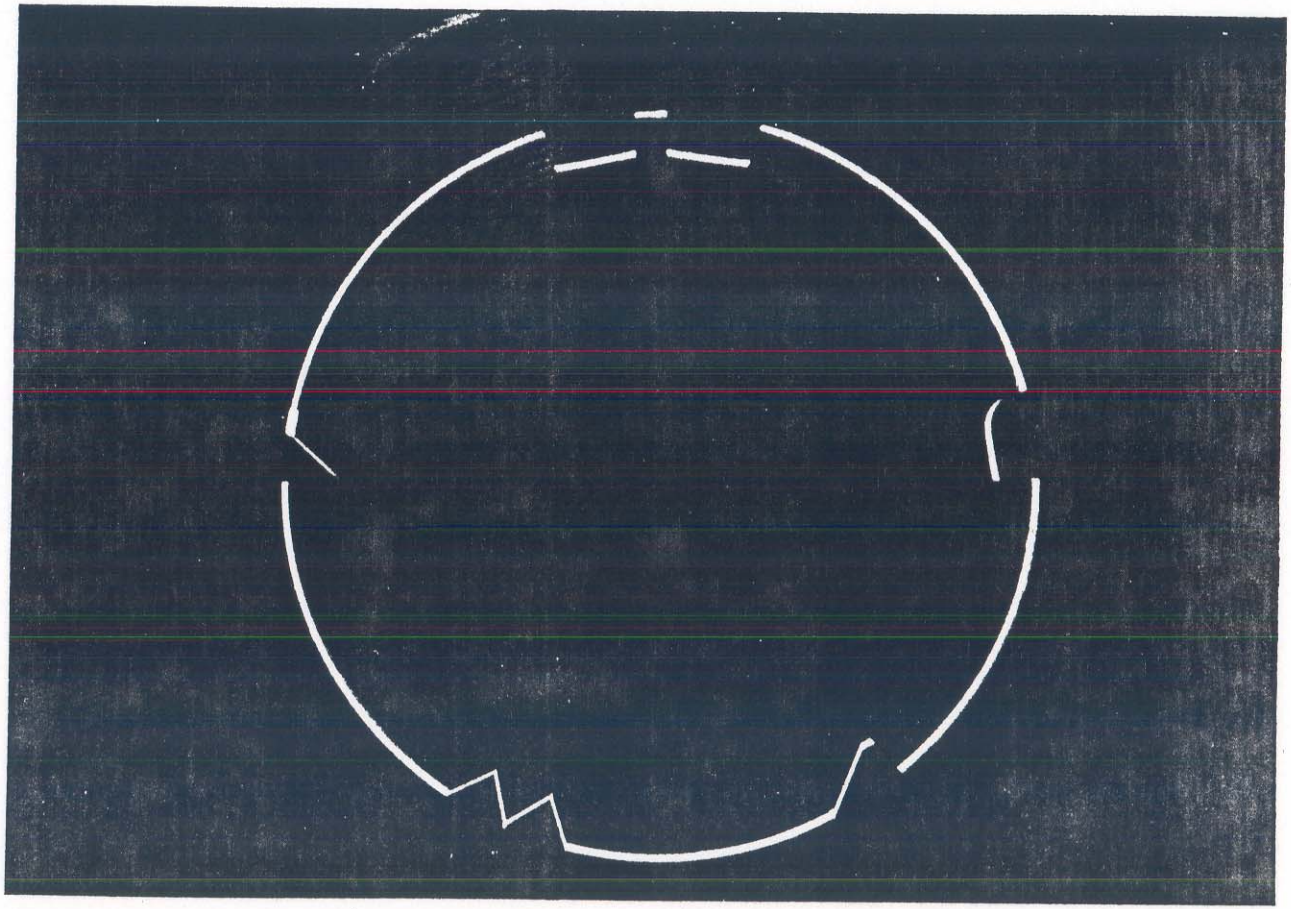

Figure 7

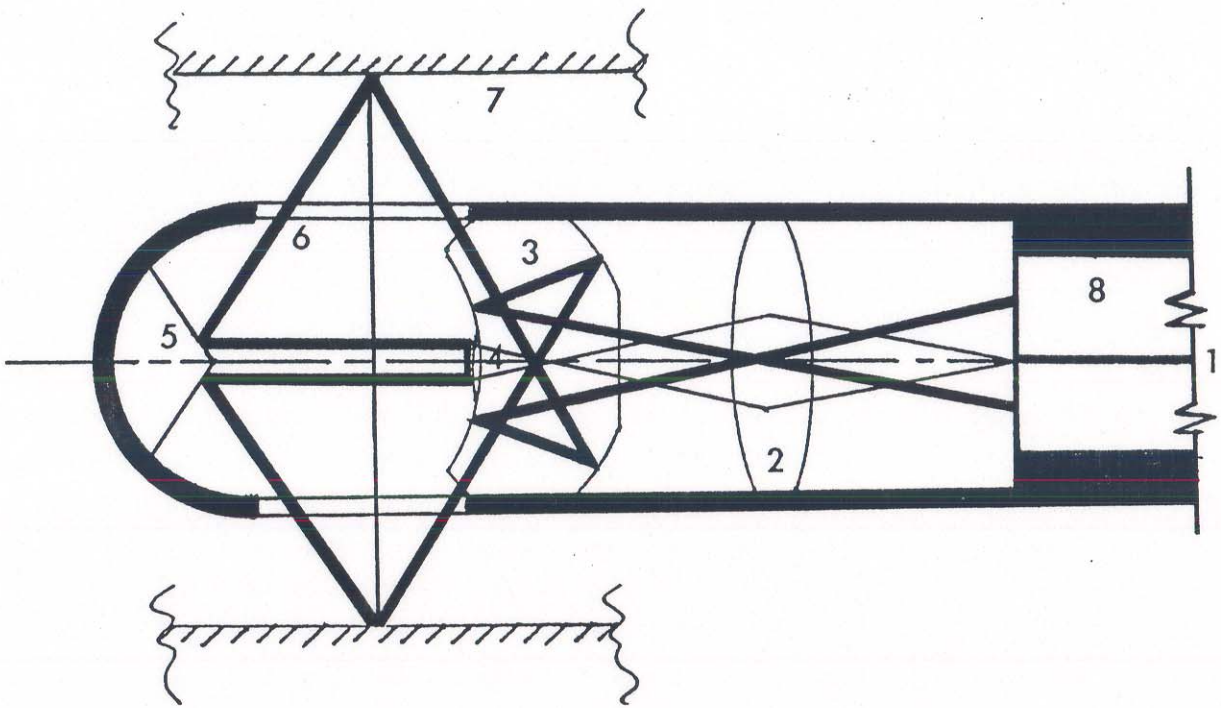

1. ILLUMINATING FIBER FROM LASER
2. PROJECTION LENS
3. PANORAMIC DOUGHNUT LENS
4. COLLIMATING LENS WITH MASK
5. CONICAL MIRROR
6. TRANSPARENT WINDOW
7. TEST OBJECT
8. IMAGE BUNDLE TO COMPUTER